Optimization of Thermal Processes Applied to Hypoeutectic White Cast Iron containing 25% Cr Aimed at Increasing Erosive Wear Resistance

Alejandro Gonzalez-Pociño[ID]**, Florentino Alvarez-Antolin ***[ID] **and Juan Asensio-Lozano**[ID]

Materials Pro Group, Departamento de Ciencia de los Materiales e Ingeniería Metalúrgica, Universidad de Oviedo, Independencia 13, 33004 Oviedo, Spain; gonzalezpalejandro@uniovi.es (A.G.-P.); jasensio@uniovi.es (J.A.-L.)

* Correspondence: alvarezflorentino@uniovi.es; Tel.: +34-985-181-949

check for
updates

Abstract: Hypoeutectic white cast irons containing 25% Cr are used in very demanding environments that require high resistance to erosive wear, for instance, the crushing and processing of minerals or the manufacture of cement. This high percentage in Cr, in turn, favors corrosion resistance. The application of a Design of Experiments (DoE) allows the analysis of the effects of modifying certain factors related to the heat treatments applied to these alloys. Among these factors, the influence of prior softening treatment to facilitate the machining of these cast irons and the influence of the factors related to the destabilization of austenite, during both quenching and tempering, were analyzed. The precipitated phases were identified by X-ray diffraction (XRD), while the Rietveld structural refinement method was used to determine their percentages by weight. Erosive wear resistance was calculated using the ASTM G76 standard test method. It is concluded that the thermal softening treatment, consisting of 2 h at 1000 °C and 24 h at 700 °C, does not result in additional softening of the material compared to its as-cast state. Furthermore, it is observed that not only eutectic carbides influence wear resistance, but that the influence of the matrix constituent is also significant. It is also verified that the tempering treatment plays a decisive role in wear resistance. Temperatures of 500 °C and tempering times of 6 h increase the wear resistance and hardness of the aforementioned matrix constituent. Tempering temperatures of 200 °C lead to an increase in retained austenite content and the presence of M_3C carbides versus mixed M_7C_3 and $M_{23}C_6$ carbides. The quench cooling medium is not found to have a significant influence on the hardness or wear resistance.

Keywords: high-Cr white cast irons; Rietveld structural refinement; erosive wear resistance; destabilization of austenite; secondary carbides; tempering

1. Introduction

High-Cr white cast irons are widely used to withstand abrasive and erosive wear in applications such as the crushing and processing of minerals, cement manufacturing, and the pumping of sludge generated in these industries [1,2]. These alloys usually contain between 15 and 30% Cr [1]. Wear resistance increases as the percentage of chromium increases [3]. The type and distribution of eutectic or secondary carbides depend on the composition of the alloy and the heat treatments it is subjected to [1]. To enhance the wear resistance of these cast irons, it is advisable to carry out a treatment to destabilize the austenite [4]. The destabilization of austenite requires long dwell times at the austenitization temperature, due to the high concentration of alloy elements in the austenite crystalline cell, which hinders the diffusion of carbon. With increasing dwell time at the destabilization temperature, two kinetics simultaneously compete with one another: On the one hand, the dissolution of eutectic

carbides that have formed as a result of non-equilibrium solidification and, on the other, an increase in the amount of precipitated secondary carbides [5]. Excessive dwell times can lead to the thickening of these secondary carbides [6]. Eutectic carbides are always of the M_7C_3 type, also called K_2 carbides. However, depending on the chromium content, the secondary carbides can be of the M_7C_3 type and the $M_{23}C_6$ type also called K_1 carbides [1,7–10]. Besides precipitating during the austenite destabilization treatment, secondary carbides can precipitate during tempering [11]. Carpenter et al. conclude that the majority of secondary carbides precipitated in cast irons with 26% Cr are of type K_1, which would have a cubic structure with a mesh parameter of 1.04 nm [12].

The matrix phase of these cast irons is austenite, which explains why they show greater toughness than Ni-hard cast irons [7,13,14]. This austenite has a high hardenability that allows its transformation into martensite by means of simple air cooling [15]. Erosive wear resistance fundamentally depends on the behavior of the matrix constituent, made up of austenite and secondary carbides [2]. The hardness of K_2 carbides falls within the 1500–1800 HV range, so the hardness of the matrix constituent exceeds that of most abrasive materials, particularly corundum (1300 HV) and quartz (800–1000 HV). Only SiC (2500 HV) would exceed it in terms of hardness [16]. From all the above, it follows that erosive wear of these carbides would not occur, but rather their detachment when the surrounding phase becomes worn [17]. Cast irons with a very high percentage in Cr are those that show greater resistance to oxidation and corrosion. In particular, Cr/C ratios close to or greater than 10 are found to be favorable [18]. This group of wear- and corrosion-resistant Cr-rich alloy cast irons would include those with a Cr content of around 25% and a C content of around 2.5–2.8%.

The aim of this study is to optimize the erosive wear resistance of a white cast iron containing 25% Cr by the application of a Design of Experiments (DoE). For this purpose, the difference in results obtained via the controlled variation of the process parameters related to the applied heat treatments is measured and analyzed. The aim is to correlate the results with the microstructural variations the material undergoes following these process modifications. In particular, parameters related to the destabilization of austenite, the quench cooling medium, and the tempering conditions are analyzed. Table 1 shows the chemical composition of this white cast iron. The research methodology followed was the application of a fractional DoE, in which six factors were analyzed, performing eight experiments in all [19]. The results will allow manufacturers of this material to design the most suitable heat treatment so that the material offers high wear resistance in the aforementioned industries.

Table 1. Chemical Composition (% by weight).

C	Si	Mn	Cr	Mo
2.7	1.2	0.8	25.1	0.5

2. Materials and Methods

Via the application of a DoE, the aim is to modify certain manufacturing parameters in a deliberate and controlled manner so as to analyze the variations produced in the properties of the material. In this case, the aim is to analyze the variations in the erosive wear resistance and microstructure of the material so as to subsequently correlate in-service performance with these microstructural changes. Statistical analysis of the variations in the responses of the material enables us to determine which of the analyzed factors has a significant effect on its wear resistance. Table 2 shows the analyzed factors and the levels of analysis in each of these factors. Among the factors listed in Table 2, the meaning of factor C needs clarifying. This is a softening treatment aimed at facilitating the machining of this material before the hardening treatment [20]. This heat treatment consisted of 2 h at 1000 °C and 24 h at 700 °C. The goals of this treatment would be to destabilize the retained austenite and to seek a majority presence of perlite, thus facilitating hypothetical machining should it be necessary for the manufacture of industrial components using this material. The proposed dwell times at the destabilization temperature of austenite in the quenching process, Factor B, are higher than usual.

The redissolution of any possible cementite carbides precipitated during the softening treatment is, thus sought, thereby favoring the precipitation of Cr-rich secondary carbides and an increase in the Ms temperature so as to avoid the presence of retained austenite as far as possible after quenching [20].

Table 2. Factors and Levels.

	Factors		Levels	
Code	**Metallurgical Parameter**		**Level −1**	**Level +1**
A	Destabilization temperature of austenite (°C)		1000	1100
B	Dwell time at the destabilization temperature of austenite (h)		4	8
C	Softening treatment prior to hardening		yes	no
D	Quench cooling medium		air	oil
E	Tempering temperature (°C)		200	500
F	Tempering dwell time (h)		3	6

The effect of a factor is defined as the variation in certain property of the material as a result of the variation of said factor. The property of the material may be the wearing resistance, hardness, the volume fraction of retained austenite, et cetera. This type of effect is called the main effect. Sometimes, the effect of one factor depends on the value that another takes. When this occurs, these factors are said to interact. The influence of the main effects on the variations in the response of the material is greater than that of the two-factor interactions. In turn, the influence of the two-factor interactions is greater than that of the three-factor interactions, and so on successively. In industrial practice, it is sufficient to take into account the main effects and two-factors interactions. This simplification allows for reducing the number of experiments. In this study, the effect of six factors with eight experiments has been analyzed. If the aim were to analyze all the possible interactions, it would be necessary to perform 64 experiments ($2^6 = 64$). In the case in hand, however, only eight effects (2^{6-3}) have been estimated, which means a 1/8 (64/8 = 8) fractional factorial design. Table 3 shows the array of experiments thus generated to carry out a DoE with six factors, two levels for each factor, and eight experiments. Columns D, E, and F have been, respectively, constructed from the product of columns A × B, A × C, and B × C. The "Restricted Confounding Pattern" column indicates only the main effects and those 2-factor interactions whose effects are confounded with the main effects. The main effects and interactions may be associated with the terms of a Taylor series of the response function. Hence, by excluding third-order interactions, the third-order terms of the Taylor series would likewise be excluded. This allows performing fractional DOEs, reducing the number of experiments, but assuming a possible error resulting from excluding interactions between factors. The confounding pattern should include all the effects confounded with each other. However, Table 3 shows a restricted confounding pattern in which only the main effects and the two-factor interactions are represented. The aim of using a fractional approach is not to achieve a good fit, but to try to determine which factors have a significant effect on the response variable.

Table 3. The array of Experiments.

Experiment	A	B	C	D = A × B	E = A × C	F = B × C	Restricted Confounding Pattern
1	−1	−1	−1	+1	+1	+1	A + BD + CE
2	+1	−1	−1	−1	−1	+1	B + AD + CF
3	−1	+1	−1	−1	+1	−1	C + AE + BF
4	+1	+1	−1	+1	−1	−1	D + AB + EF
5	−1	−1	+1	+1	−1	−1	E + AC + DF
6	+1	−1	+1	−1	+1	−1	F + BC + DE
7	−1	+1	+1	−1	−1	+1	AF + BE + CD
8	+1	+1	+1	+1	+1	+1	

The effects are linear combinations of the analyzed responses. Hence, applying the central limit theorem (CLT), they will follow a normal law. If we represent the distribution function of the N

(0,σ) law on the normal probability plot scale, it will take the form of a straight line. This line must necessarily pass through the coordinate point (0.50). If any calculated effect followed a different normal law, e.g., N (μ,σ′), it would not appear aligned along this line. Those effects that deviate from the straight line towards the ends on the normal probability plot are considered significant. For example, if an effect deviates to the left, this would indicate that the factor associated with this effect at its −1 level would increase the value of the response. Similarly, if an effect deviates to the right of the straight line, this would indicate that the factor associated with this effect at its +1 level would increase the value of the response. The statistical analysis was carried out with the help of the Statagraphics Centurion XVI program, version 16.1.18.

The wear resistance, hardness, and hardness of the matrix constituent were analyzed via the eight experiments listed in Table 3. The aim of the last analysis was to test whether the wear resistance of the material might have some kind of relationship with the hardness of the matrix constituent. Moreover, the possible relationship between the microstructure obtained in these experiments and the wear resistance of the material was likewise analyzed. The analyzed responses were:

- Vickers hardness of the material. The applied load was 300 N, while the hardness value was the average value obtained from 10 indentations.
- The Vickers hardness of the constituent matrix. In this case, the applied load was 0.5 N, while the hardness value was calculated as the average value obtained from 10 indentations.
- Erosive wear resistance. This test was carried out as per ASTM G76 [21] by means of compressed air blasting with corundum particles, applying a pressure of 2 bar, a flow rate of 250 g/min and a 30° angle of incidence on the sample surface. The times employed in each experiment were 2, 4, and 6 min. Three repetitions were performed per test. The weight loss per unit time (mg/min) was determined from the average values obtained at each test time. As noted in the aforementioned standard, the results are shown in mm^3 of material loss per gram of abrasive (mm^3/g).
- The following microstructural variables:

  o   percentage by weight of austenite
  o   percentage by weight of martensite
  o   percentage by weight of carbides
  o   volume of the austenite crystal cell

The microstructural variables were determined by X-ray diffraction on a SEIFERT XRD 3000 T/T diffractometer (Baker Hughes, Celle, Germany). The radiation was emitted via a fine-focus Mo tube at a working power of 40 kV × 40 mA and monochromatized to the Kα doublet: λ_1 = 0.7093616 Å and λ_2 = 0.713607 Å. The diffracted intensity was determined in a 2θ range from 7 to 57° with an angular step and counting time of approximately 0.03° and 22 s, respectively. To calibrate the equipment, the position of the reflections and the profiles of the associated Bragg peaks were calibrated with the National Institute of Standards and Technology (NIST) Si (640C) standard and LaB6 (660a) standard, respectively. The Rietveld structural refinement method was used to determine the percentage of the crystalline phases via fitting of the diffractograms. To this end, following the recording of the diffraction figures, a structural refinement was carried out using the crystallographic information files present in the Inorganic Crystal Structure Database (ICSD), FIZ Karlsruhe, Germany. The program employed for this purpose was FullProf.2k, version 6.20 (2018). The increase in width observed in the peaks of the majority phases were modeled using Stephens' formulation [22], which is implemented in the aforementioned analysis program.

3. Results

Figure 1 shows the microstructure of these cast irons in the as-cast state following solidification in a sand mold. This microstructure is mainly made up of eutectic carbides of the K_2 type, retained austenite and pearlite. The proeutectic austenite presents a dendritic growth model. The presence of

the eutectic constituent can be observed between these dendrites. The hardness of the cast iron in this state was 305 HV.
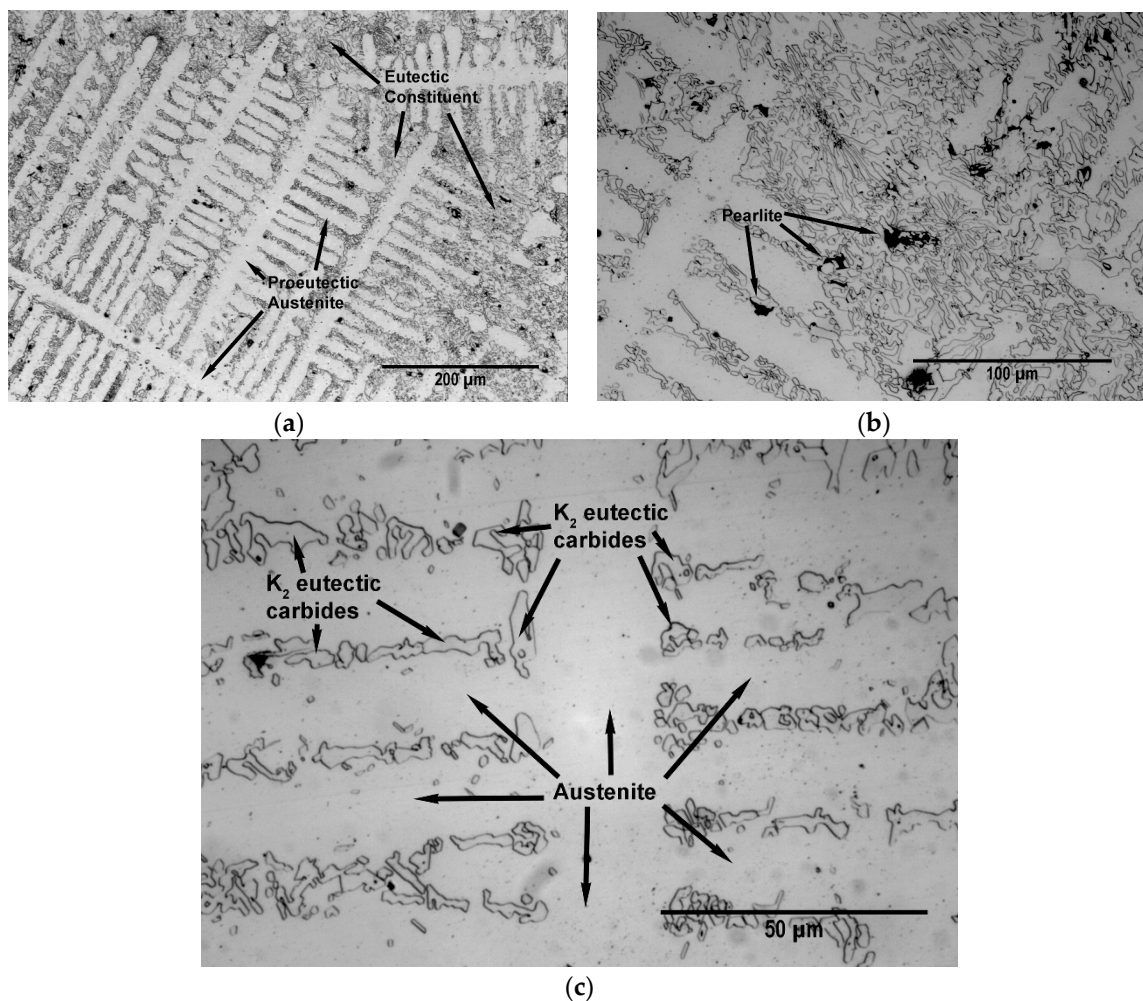

Figure 1. As-cast microstructure: (**a**) ×200 magnification; (**b**) ×500 magnification; (**c**) ×1000 magnification.

One of the analyzed factors was the effect of a possible softening treatment designed to facilitate machining of this material with chip removal [20]. Figure 2 shows the microstructure obtained following this treatment. Coalescence and thickening of the secondary carbides precipitated during the destabilization of austenite, prior to the isothermal dwell time at 700 °C, can be observed [20,23]. However, the measured hardness in this state reached an average value of 360 HV, which was greater than of the as-cast state. This reason for this could be the high volume fraction of retained austenite that these cast irons present in said as-cast state [24]. From all the above, it follows that if the aim were to machine this material before its hardening by heat treatment, it would not be necessary to perform a prior softening treatment, contrary to what was concluded in a previous study on white cast irons containing 18% Cr.

Table 4 shows the results obtained from the analysis of:

- the overall hardness of the material
- the hardness of the constituent matrix, whose microstructure is a consequence of the destabilization of austenite and its transformation
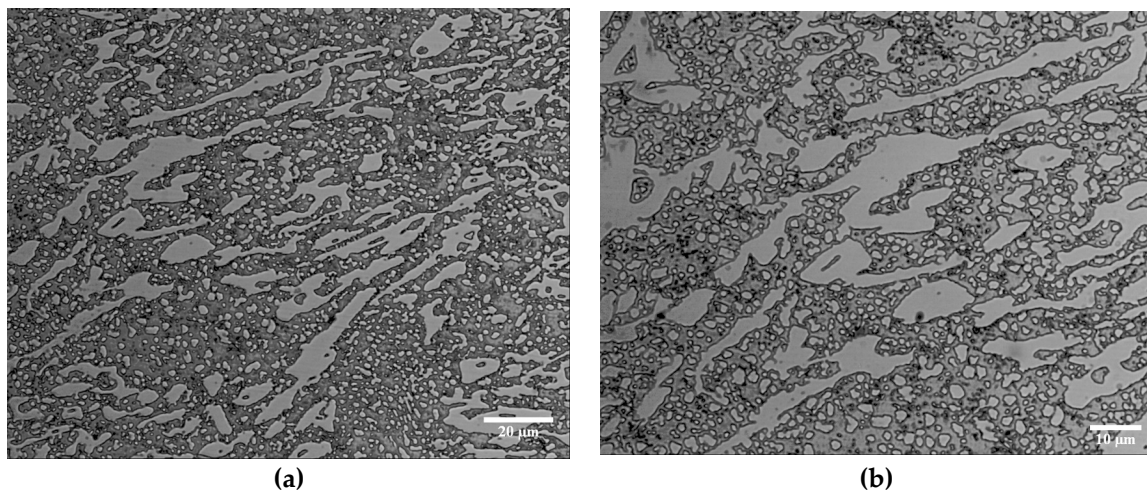- the weight loss in the erosive wear test.

(a)　　　　　　　　　　　　　　　　　　　　　　**(b)**

Figure 2. Microstructure following the softening treatment: (**a**) 400× magnification; (**b**) 600× magnification.

Table 4. Hardness and weight loss in the erosive wear test.

No.	Hardness		Microhardness		Weight Loss		Calculated Effects
	HV (300 N)	Effect	HV (0.5 N)	Effect	mm^3/g × 10^6	Effect	
1	613	664.62	570	550.75	14.5	21.73	Average
2	655	64.25	570	−0.5	19.5	1.57	A + BD + CE
3	642	15.75	597	2.5	25.1	3.57	B + AD + CF
4	670	39.25	459	3.5	25	1.27	C + AE + BF
5	639	2.75	498	−31.5	25.1	−0.87	D + AB + EF
6	720	29.25	560	68.5	20.7	−4.47	E + AC + DF
7	636	−6.25	539	44.5	19.1	1.42	F + BC + DE
8	742	9.75	613	37.5	24.1	3.82	AF + BE + CD

Figure 3 shows the representation of these effects on a normal probabilistic plot, highlighting those that have a significant influence on the analyzed responses.

Figure 3a shows that factors A and E (destabilization temperature of austenite and tempering temperature) have a significant effect on the hardness of the material. Placing these two factors at their +1 level (1100 °C and 500 °C, respectively) would result in an increase in hardness. It can further be seen that some of the AE and BF interactions would have a significant effect on hardness. Table 5 shows the results of the analysis of these interactions. It can be seen that the interaction that produces a greater increase in hardness is AE when both factors are placed at their +1 level.

Table 5. Analysis of the effects of interactions AE and BF on the hardness of the material.

AE	−1	+1	BF	−1	+1
−1	638	613	**−1**	680	634
+1	663	**731**	**+1**	656	689

Figure 3b shows that E (tempering temperature) and F (tempering time) are the factors that have a significant effect on the hardness of the matrix constituent. An increase in this hardness would be achieved by placing these two factors at their +1 level (500 °C and 6 h, respectively). From these results, it may be deduced that a high tempering temperature and long tempering times favor a second destabilization of the retained austenite. The significant effect of interactions AF and BE can also be appreciated. Table 6 shows the results of the analysis of these two interactions. It follows that the effect of factor F is favored when factor A (destabilization temperature of austenite) is placed at its +1 level (1100 °C). Similarly, it follows that the effect of factor E is favored when factor B (dwell time at the destabilization temperature) is placed at its +1 level (8 h).

**Table 6.** Analysis of the effects of interactions AF and BE on the hardness of the matrix constituent.

AE	−1	+1	BF	−1	+1
−1	547	555	**−1**	534	565
+1	509	**592**	**+1**	499	**605**

Figure 3c shows that factors E (tempering temperature) and F (tempering time) have a significant effect on erosive wear resistance. Placing both factors at their +1 level (500 °C and 6 h, respectively) would result in an increase in wear resistance. It should be noted that these same factors are those that have a significant influence on the hardness of the matrix constituent, thus corroborating the importance of this constituent with respect to the wear resistance.

It should also be noted that the quench cooling medium is not found to have a significant influence either on the hardness or wear resistance of the material.

Figure 4 shows the diffractograms obtained in the eight experiments, highlighting the main identified phases.

Figure 5 shows the overall fittings using the Rietveld method. The red marks indicate the observed intensities; the black line, the intensity calculated according to the Rietveld structural model; the blue line, the difference between the two, while the vertical segments indicate the angular positions of the different identified phases.
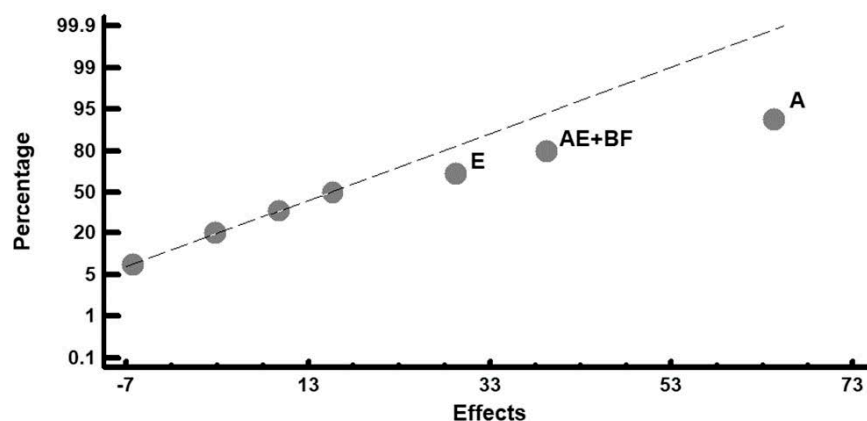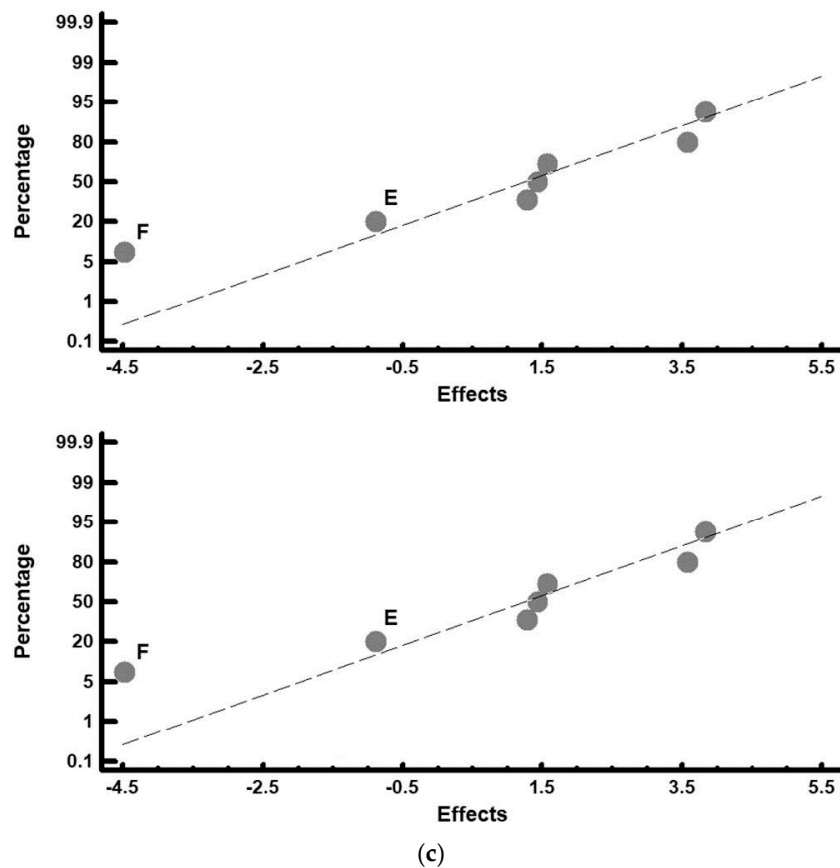

(a)
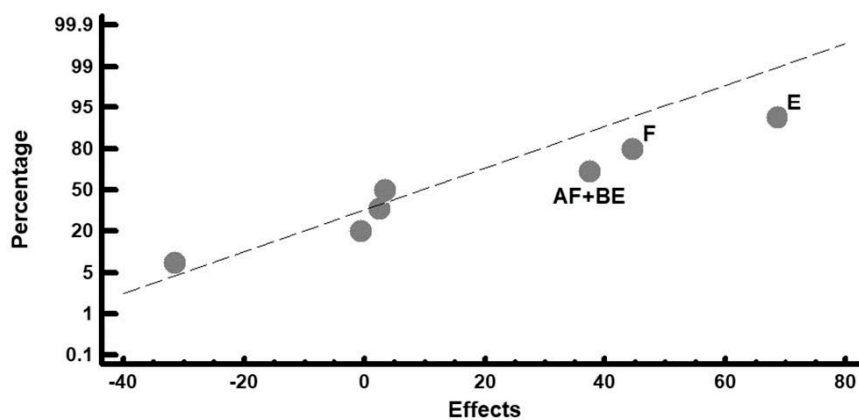
(b)

Figure 3. *Cont.*

Figure 3. Representation of the effects on a normal probability plot. Those factors with a significant effect on the analyzed responses are highlighted. (**a**) overall hardness; (**b**) hardness of the matrix phase; (**c**) weight loss in the erosive wear test (mm^3/g × 10^6).
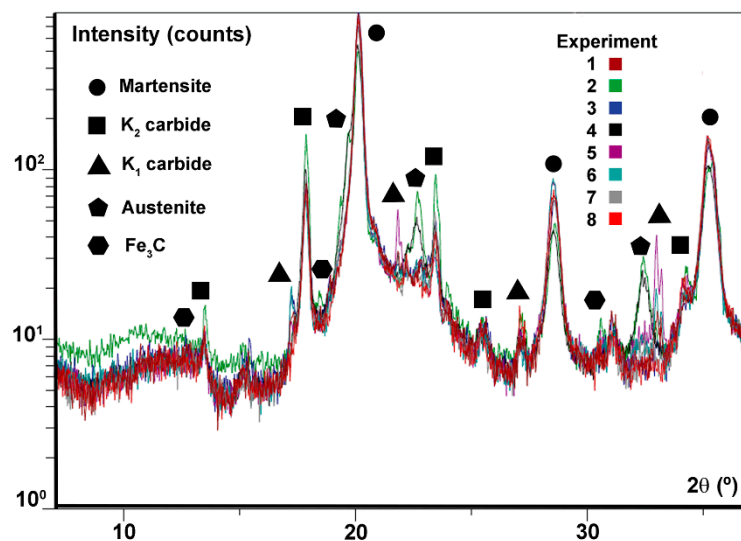

Figure 4. Superimposed diffractograms obtained in the eight experiments.

Table 7 shows the percentages by weight and the mesh parameters of the main crystalline phases detected by XRD. The goodness-of-fit is defined by factor Rwp, index Rexp, and the ratio of their squares, Chi^2 = (Rwp/Rexp)^2.

Table 7. Microstructural parameters, weight distributions of the precipitated phases, and volume of austenite. The statistical error is given between parentheses.

Experiment	Rietveld Fitting	Phases	a (Å)	b (Å)	c (Å)	wt. %
1	Rwp = 13.6 Rexp = 7.94 Chi^2 = 2.95	Martensite	2.87106 (0.0005)		2.88359 (0.0010)	44.5 (4.5)
		K$_2$ carbides	4.49539 (0.0157)	7.00445 (0.0079)	12.09299 (0.0081)	53.5 (6.8)
		K$_1$ carbides	10.60637 (0.0008)			0.7 (0.5)
2	Rwp = 14.9 Rexp = 6.8 Chi^2 = 4.80	Martensite	2.86693 (0.0009)		2.88730 (0.0011)	13.1 (1.1)
		Austenite	3.60039 (0.0006)			9.0 (0.7)
		K$_2$ carbides	4.50051 (0.0036)	6.99363 (0.0035)	12.09151 (0.0037)	75.9 (4.6)
		Fe$_3$C	4.84209 (0.0029)	6.79065 (0.0041)	4.41551 (0.0023)	2.0 (0.5)
3	Rwp = 15.2 Rexp = 7.85 Chi^2 = 3.76	Martensite	2.87043 (0.0005)		2.88247 (0.0011)	42.5 (3.3)
		K$_2$ carbides	4.49884 (0.0166)	7.00169 (0.0081)	12.09704 (0.0083)	56.6 (7.1)
		K$_1$ carbides	10.60637 (0.0008)			0.9 (0.4)
4	Rwp = 11.2 Rexp = 5.85 Chi^2 = 3.65	Martensite	2.87520 (0.011)		2.89022 (0.0015)	26.0 (1.5)
		Austenite	3.59992 (0.0009)			7.3 (0.9)
		K$_2$ carbides	4.49662 (0.0098)	7.00633 (0.0062)	12.11956 (0.0067)	65.3 (5.4)
		K$_1$ carbides	10.60637 (0.0008)			0.1 (0.1)
		Fe$_3$C	4.84209 (0.0029)	6.79065 (0.0041)	4.41551 (0.0023)	1.3 (0.5)
5	Rwp = 14.0 Rexp = 7.02 Chi^2 = 3.98	Martensite	2.87064 (0.0004)		2.88780 (0.0006)	31.0 (2.0)
		K$_2$ carbides	4.49496 (0.0057)	7.00124 (0.0073)	12.11749 (0.0092)	48.9 (3.5)
		K$_1$ carbides	10.60637 (0.0008)			18.8 (1.7)
		Fe$_3$C	4.84209 (0.0029)	6.79065 (0.0041)	4.41551 (0.0023)	1.3 (0.6)
6	Rwp = 11.9 Rexp = 7.54 Chi^2 = 2.49	Martensite	2.87125 (0.0005)		2.88696 (0.0009)	47.5 (4.2)
		K$_2$ carbides	4.49711 (0.0098)	7.00760 (0.0064)	12.10338 (0.0069)	52.5 (5.6)
7	Rwp = 12.7 Rexp = 7.88 Chi^2 = 2.61	Martensite	2.87138 (0.0004)		2.88712 (0.0007)	40.4 (3.8)
		K$_2$ carbides	4.49164 (0.0064)	7.01520 (0.0064)	12.10307 (0.0079)	53.3 (5.0)
		K$_1$ carbides	10.60637 (0.0008)			5.5 (1.5)
		Fe$_3$C	4.84209 (0.0031)	6.79065 (0.0043)	4.41551 (0.0028)	0.8 (0.4)
8	Rwp = 11.2 Rexp = 7.01 Chi^2 = 2.56	Martensite	2.87225 (0.0006)		2.89017 (0.0011)	45.4 (3.2)
		K$_2$ carbides	4.50240 (0.0089)	7.00719 (0.0057)	12.10593 (0.0065)	54.6 (5.4)

Table 8 shows the average values obtained in each experiment, together with the effects corresponding to the restricted confounding pattern specified in the array of experiments. The row corresponding to the average shows the average value obtained for each of the analyzed responses.

Figure 6 shows the representation of these effects on a normal probability plot, highlighting those that have a significant effect on these responses.

Table 8. Average values and effects obtained for the phases present in the material.

Experiment	Martensite		Austenite		Calculated Effects
	(wt.%)	Effect	(wt.%)	Effect	
1	44.77	36.3463	-	2.0337	Average
2	13.09	−6.682	9.01	4.067	A + BD + CE
3	42.54	4.507	-	−0.437	B + AD + CF
4	26	9.492	7.26	−4.067	C + AE + BF
5	31.02	0.922	-	−0.437	D + AB + EF
6	47.49	17.427	-	−4.067	E + AC + DF
7	40.42	−0.832	-	0.437	F + BC + DE
8	45.44	−6.647	-	0.437	AF + BE + CD

(**a**) Percentage by weight of martensite and austenite.

Experiment	K_1 Carbides		K_2 Carbides		Fe_3C		Calculated Effects
	(wt.%)	Effect	(wt.%)	Effect	(wt.%)	Effect	
1	0.75	3.251	53.47	57.56	-	0.6787	Average
2	–	−6.45	75.87	9.01	2.03	0.302	A + BD + CE
3	0.87	−3.27	56.59	−0.24	-	−0.307	B + AD + CF
4	0.10	5.64	65.35	−10.51	1.29	−0.302	C + AE + BF
5	18.8	3.32	48.89	−3.99	1.30	−0.062	D + AB + EF
6	–	−5.69	52.51	−6.56	-	−1.357	E + AC + DF
7	5.49	−3.38	53.28	3.46	0.81	0.062	F + BC + DE
8	–	3.33	54.56	2.82	-	0.307	AF + BE + CD

(**b**) Percentage by weight of carbides.

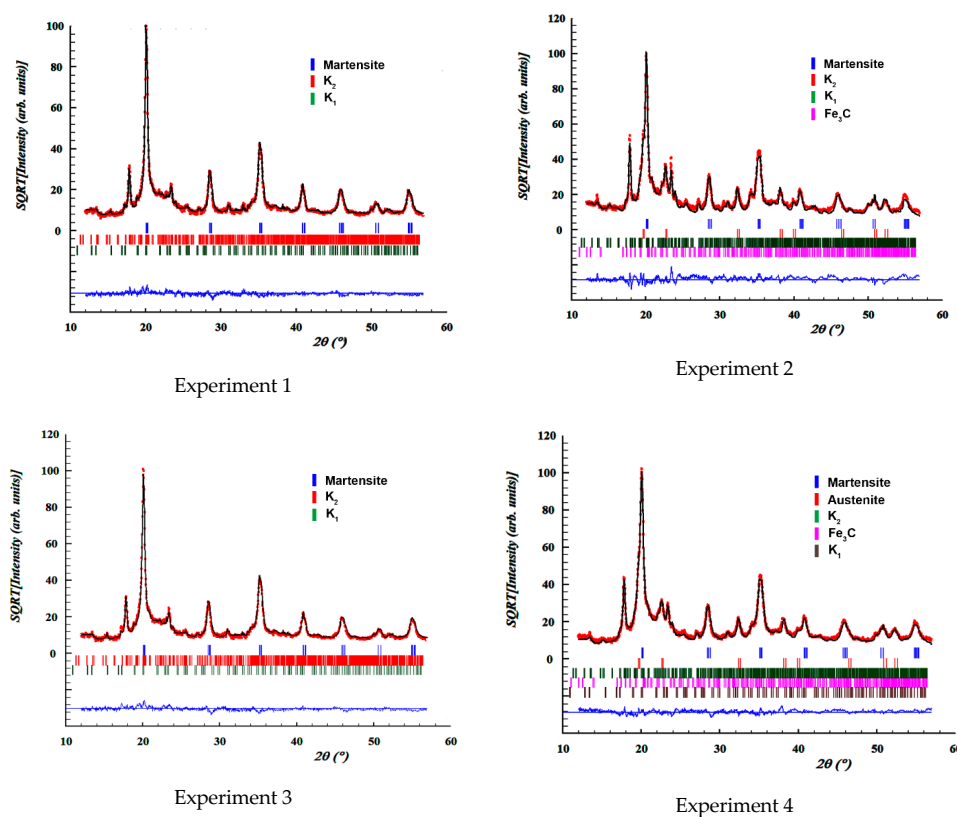Experiment 1

Experiment 2

Experiment 3

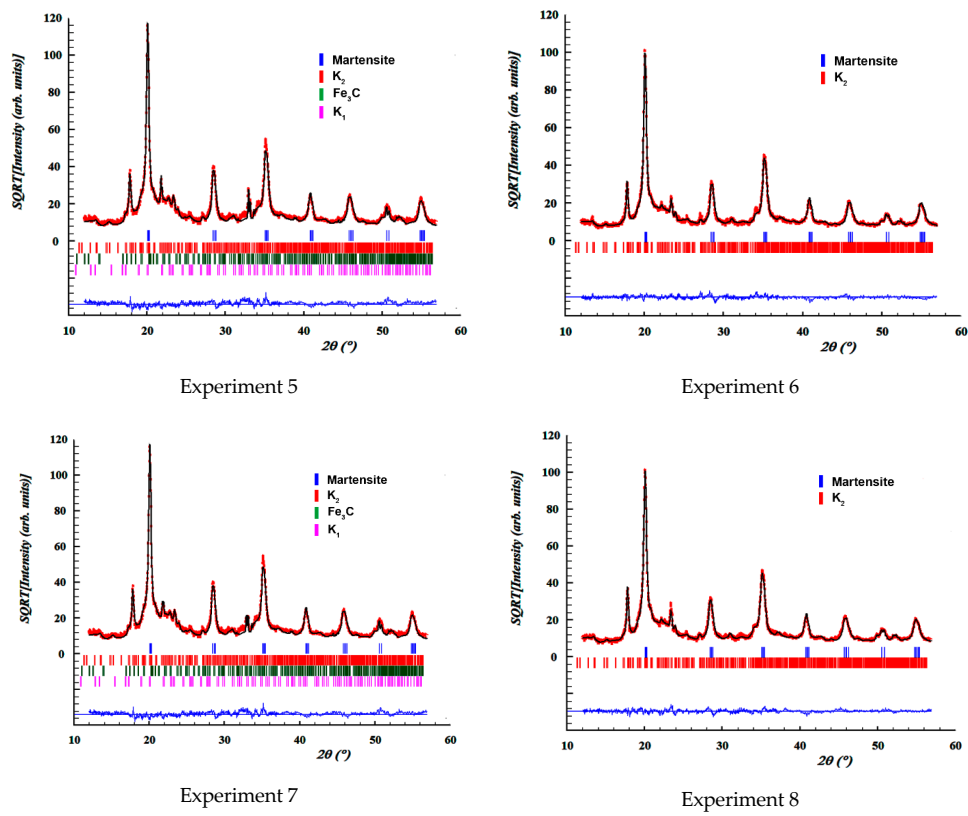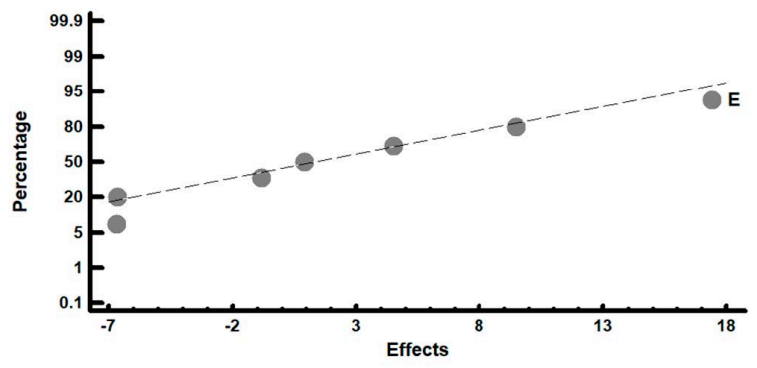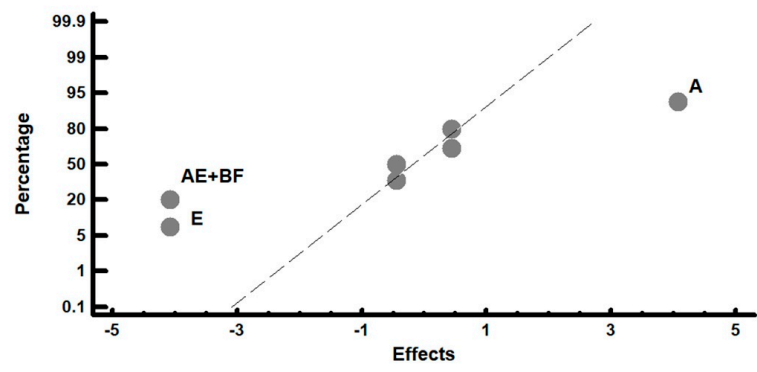Experiment 4

Figure 5. *Cont.*

Figure 5. Overall fittings using the Rietveld method. The red marks define the observed intensities.
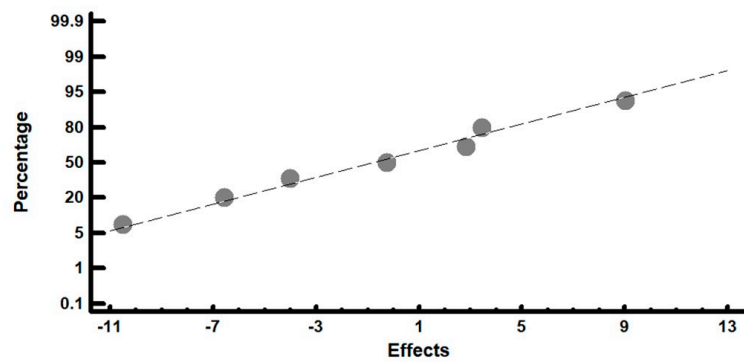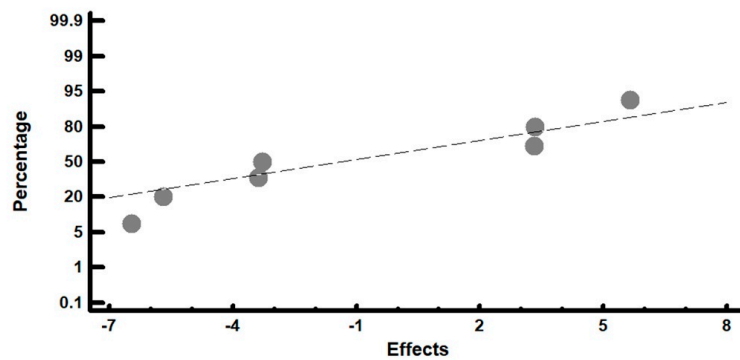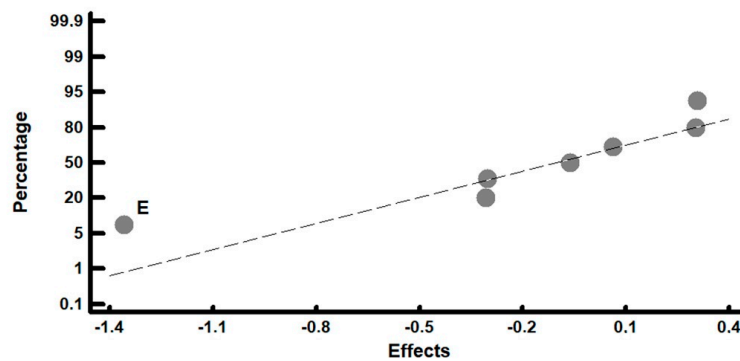

(**a**)

(**b**)

Figure 6. *Cont.*

(c)

(d)

(e)

Figure 6. Representation of the effects on the percentages by weight of the precipitated phases on a normal probability plot. Those factors with a significant effect are highlighted. (**a**) tempered martensite; (**b**) austenite; (**c**) K_2 carbides; (**d**) K_1 carbides; (**e**) Fe_3C.

Figure 6a shows that factor E (tempering temperature) has a significant influence on the percentage of tempered martensite. If the aim were to increase this content, this factor should be placed at its +1 level (500 °C). Figure 6b shows that factors A (destabilization of austenite temperature) and E (tempering temperature) have a significant effect on the percentage of retained austenite. An increase in this phase would be obtained by placing factor A at its +1 level (1100 °C) and factor E at its −1 level (200 °C). Interactions AE+BF are also found to have a significant influence. Table 9 shows the results of their analysis. It can be seen that the effect of factors A and E increase when these factors are respectively placed at their +1 and −1 level. From the XRD analysis, it is concluded that retained austenite is only observed in Experiments 2 and 4. These are the experiments in which a low tempering

temperature (200 °C) was employed. This finding is consistent with the results shown in Figure 6b and Table 9. However, a softening treatment was also employed in these experiments. Hence, it follows that the austenitization temperature at 1100 °C is high enough to dissolve precipitated carbides during this softening treatment, thereby favoring an increase in retained austenite after cooling [25]. This austenite would be destabilized when tempering at 500 °C, but not when tempering at 200 °C. Figure 7 shows the microstructure obtained after the reported softening treatment, followed by austenitization at 1100 °C for 8 h and oil cooling. It can be seen that the precipitated carbides were considerably reduced during the softening treatment compared to Figure 2. Subsequent tempering at 500 °C would remove this retained austenite.

Table 9. Analysis of the effects of interactions AE and BF on the retained austenite.

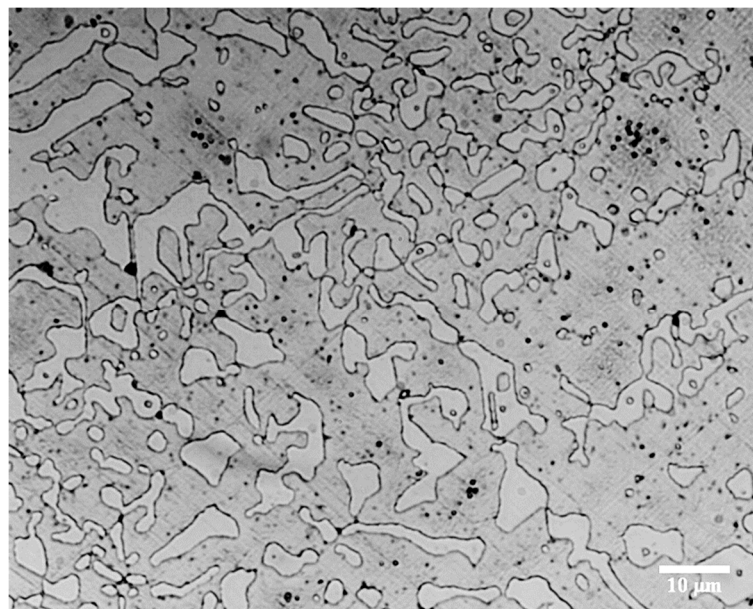| AE	−1	+1	BF	−1	+1
−1	0.00	0.00	−1	0.00	4.50
+1	8.13	0.00	+1	3.63	0.00

Figure 7. Microstructure obtained after the softening treatment, followed by austenitization at 1100 °C for 8 h and oil cooling. The redissolution of the carbides precipitated during the softening treatment can be observed.

Figure 6c,d shows that none of the factors studied in this paper (within the range of levels indicated in Table 2) have a significant effect on the percentage of K_2 or K_1 carbides. However, Figure 6e shows that factor E (tempering temperature) does have a significant effect on the percentage of Fe_3C. An increase in this phase would be achieved by placing this factor at its −1 level (200 °C). Lower temperatures are required for Fe_3C to precipitate during the tempering of the martensite, as it is only the C atoms, dissolved in a solid insert solution, which have to diffuse until reaching the crystalline defects of the cubic martensite (tempered martensite). However, the precipitation of K_1 and K_2 carbides requires a) the diffusion of Cr atoms, dissolved in a solid replacement solution, and b) the prior redissolution of Fe_3C to provide C atoms in the precipitation of these carbides. Higher temperatures are necessary for these processes to take place. In the case of the precipitation of K_1 and K_2 carbides, it is necessary to reach a temperature of 500 °C. In turn, the transformation of retained austenite into martensite is also achieved by high tempering temperatures, as evidenced by the results shown in Figure 6b. This figure also shows that high austenitization temperatures seem to favor the presence of

retained austenite, as it is found alloyed with C and Cr. This could explain why the combination of a high austenitization and low tempering temperatures favored the presence of retained austenite.

Figure 8 shows a representative micrograph of each experiment that allows us to appreciate the general microstructure of these cast irons, consisting mainly of eutectic carbides of type K1, secondary carbides of type K_1, K_2, and Fe_3C (this last carbide when tempering at low temperatures, 200 °C), tempered martensite and the possible existence of retained austenite if the tempering takes place at low temperatures (200 °C).
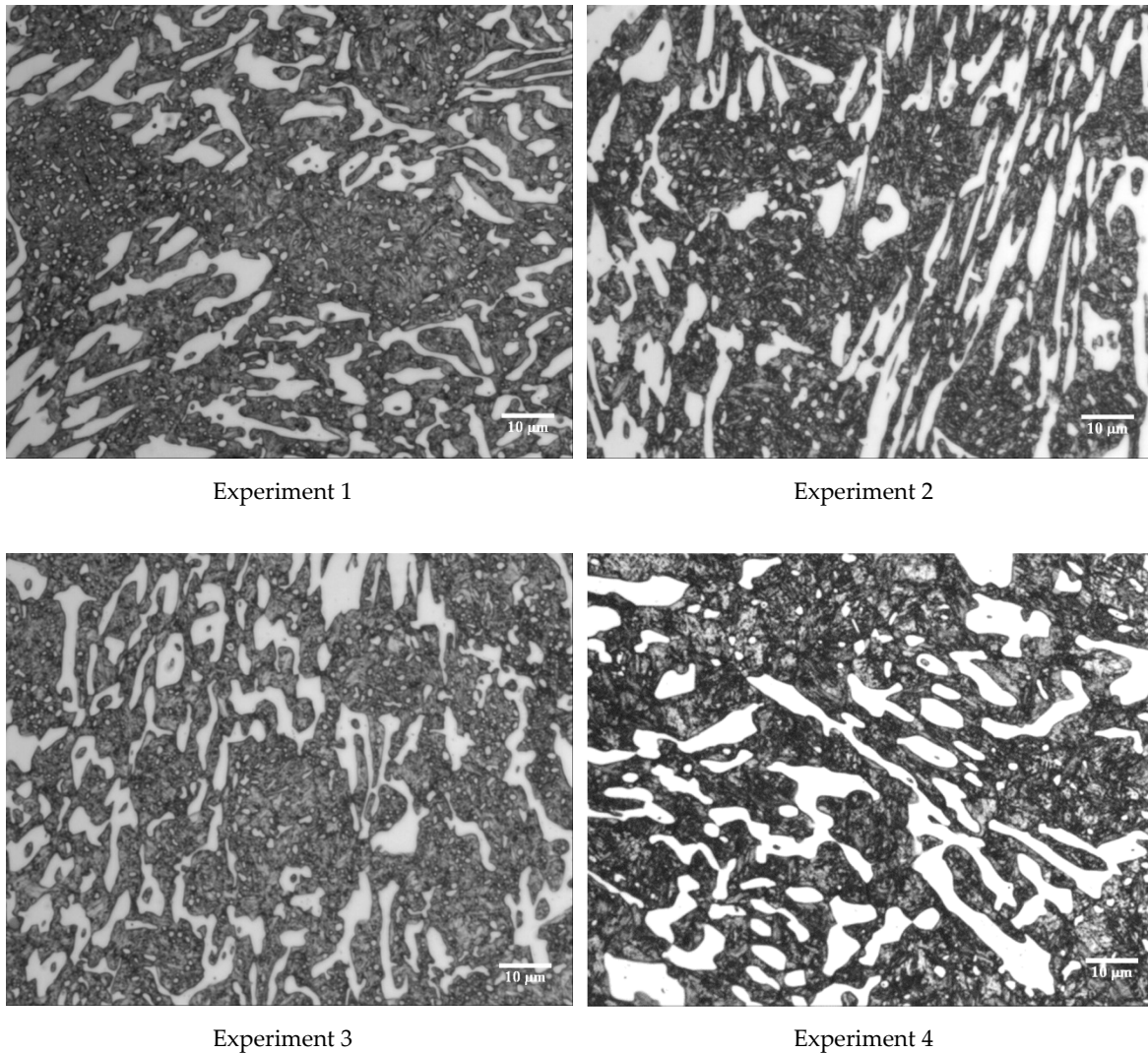

Experiment 1

Experiment 2

Experiment 3

Experiment 4

Figure 8. *Cont.*

Experiment 5

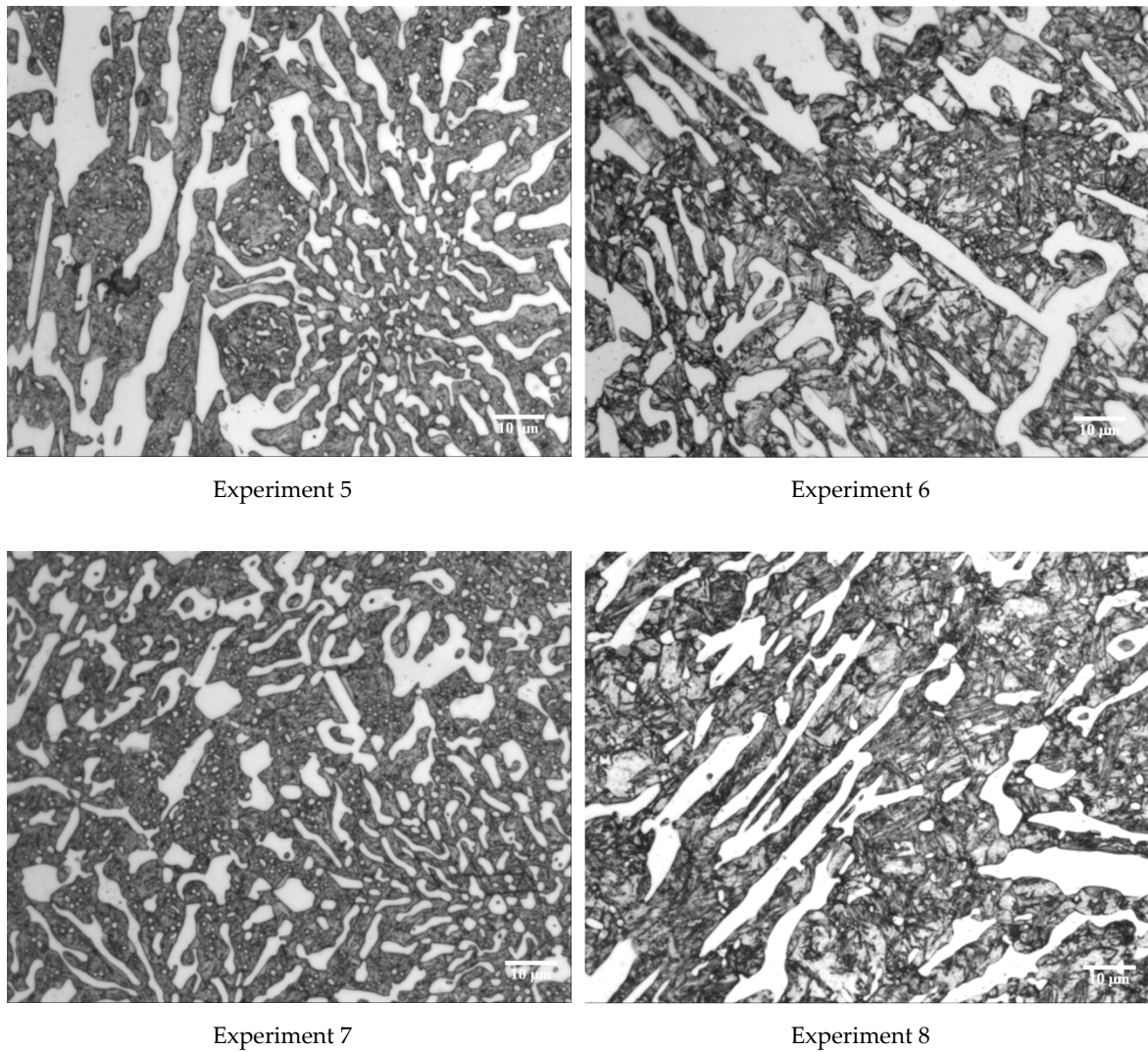Experiment 6

Experiment 7

Experiment 8

Figure 8. Representative micrographs of each of the eight experiments. All were obtained at 600× magnification.

Figure 9 shows, as a representative example, one of the tracks resulting from the wear test. In this case, the micrograph corresponds to one of the samples from Experiment 1 after 6 min of testing.
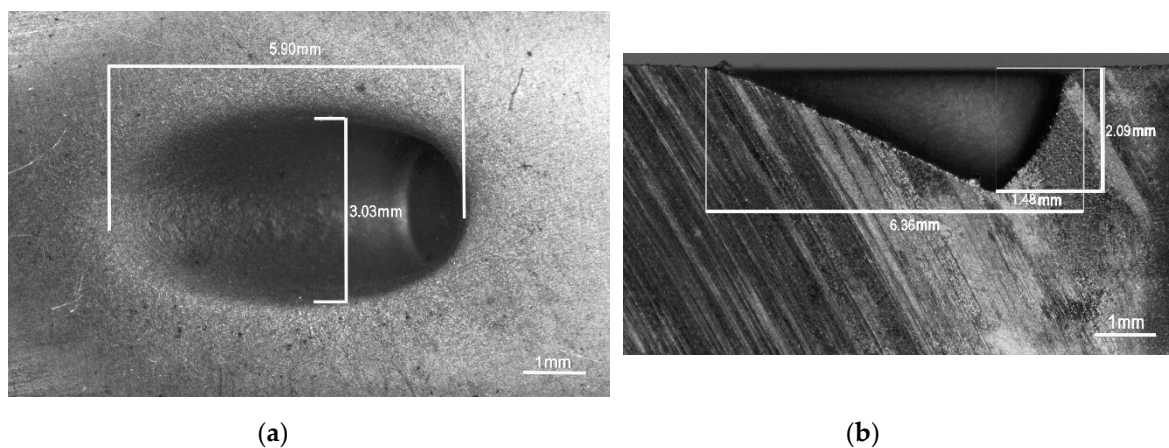

(**a**)

(**b**)

Figure 9. Geometry of the wear track. This track corresponds to one of the samples from Experiment 1 after 6 min of testing. (**a**) plan view; (**b**) side view.

4. Conclusions

The application of a Design of Experiments (DoE) allowed the analysis of the effects of modifying a variety of factors related to the heat treatments applied to hypoeutectic white cast iron containing 25% Cr on the erosive wear resistance of this material. The influence of a prior softening treatment aimed at facilitating machining of this cast iron, consisting of 2 h at 1000 °C and 24 h at 700 °C, was analyzed, as was the influence of those factors related to the destabilization of austenite. The main conclusions drawn from the study are as follows:

1. The softening heat treatment, following destabilization of the austenite, does not lead to lower hardness values with respect to the as-cast state. Isothermal softening annealing at 700 °C for 24 h following destabilization produces the coalescence and thickening of carbides that reduce the structural hardening achieved in the destabilization process.

2. An austenitization temperature of 1100 °C is high enough to redissolve the carbides precipitated during the softening treatment. After cooling, however, this favors the presence of retained austenite, which is removed if tempering is carried out at 500 °C.

3. The tempering temperature is found to be the key factor in the final percentage of martensite (α'). Tempering temperatures of 500 °C should be used to increase this percentage.

4. Following the quenching process, the tempering parameters have a significant influence on erosive wear resistance. Tempering temperatures of 500 °C and long tempering times, of around 6 h, favor an increase in wear resistance.

5. These same tempering conditions favor an increase in the hardness of the constituent matrix. This shows that it is not only the eutectic carbides that are responsible for wear resistance but that this is complemented by the resistance provided by the constituent matrix, mainly made up of tempered martensite and secondary carbides.

6. A low tempering temperature (200 °C) is not conducive to the complete transformation of the retained austenite, leading to M3C carbides being preferentially formed versus M7C3 and M23C6 carbides.

References

1. Pearce, J.T.H. Structural characterisation of high chromium cast irons. In Proceedings of the International Conference on Solidification Science and Processing: Outlook for the 21st Century, Bangalore, India, 18–21 February 2001; pp. 241–247.

2. Zhou, S.P.; Shen, Y.H.; Zhang, H.; Chen, D.Q. Heat Treatment Effect on Microstructure, Hardness and Wear Resistance of Cr26 White Cast Iron. *Chin. J. Mech. Eng.* **2015**, *28*, 140–147. [CrossRef]

3. Shimizu, K.; Purba, R.H.; Kusumoto, K.; Yaer, X.B.; Ito, J.; Kasuga, H.; Gaqi, Y.L. Microstructural evaluation and high-temperature erosion characteristics of high chromium cast irons. *Wear* **2019**, *426*, 420–427. [CrossRef]

4. Guitar, M.A.; Suarez, S.; Prat, O.; Guigou, M.D.; Gari, V.; Pereira, G.; Mucklich, F. High Chromium Cast Irons: Destabilized-Subcritical Secondary Carbide Precipitation and Its Effect on Hardness and Wear Properties. *J. Mater. Eng. Perform.* **2018**, *27*, 3877–3885. [CrossRef]

5. Gonzalez-Pocino, A.; Alvarez-Antolin, F.; Asensio-Lozano, J. Erosive Wear Resistance Regarding Different Destabilization Heat Treatments of Austenite in High Chromium White Cast Iron, Alloyed with Mo. *Metals* **2019**, *9*, 10. [CrossRef]

6. Efremenko, V.; Shimizu, K.; Chabak, Y. Effect of Destabilizing Heat Treatment on Solid-State Phase Transformation in High-Chromium Cast Irons. *Metall. Mater. Trans. A-Phys. Metall. Mater. Sci.* **2013**, *44A*, 5434–5446. [CrossRef]

7. Liu, Z.L.; Li, Y.X.; Chen, X.; Hu, K.H. Microstructure and mechanical properties of high boron white cast iron. *Mater. Sci. Eng. A-Struct. Mater. Prop. Microstruct. Process.* **2008**, *486*, 112–116. [CrossRef]

8. Antolin, J.F.A.; Garrote, L.F.; Lozano, J.A. Application of Rietveld Refinement to the correlation of the microstructure evolution of white cast irons with 18 and 25 %-wt. Cr after oil quench and successive temper treatments, with abrasive wear and bending testing. *Rev. De Metal.* **2018**, *54*, 11. [CrossRef]

9. Wang, J.; Sun, Z.P.; Zuo, R.L.; Li, C.; Shen, B.L.; Gao, S.J.; Huang, S.J. Effects of secondary carbide precipitation and transformation on abrasion resistance of the 16Cr-1Mo-1Cu white iron. *J. Mater. Eng. Perform.* **2006**, *15*, 316–319. [CrossRef]

10. Zhang, Z.G.; Yang, C.K.; Zhang, P.; Li, W. Microstructure and wear resistance of high chromium cast iron containing niobium. *China Foundry* **2014**, *11*, 179–184.

11. Liu, H.H.; Wang, J.; Yang, H.S.; Shen, B.L. Effects of cryogenic treatment on microstructure and abrasion resistance of CrMnB high-chromium cast iron subjected to sub-critical treatment. *Mater. Sci. Eng. A-Struct. Mater. Prop. Microstruct. Process.* **2008**, *478*, 324–328. [CrossRef]

12. Carpenter, S.D.; Carpenter, D.; Pearce, J.T.H. XRD and electron microscope study of a heat treated 26.6% chromium white iron microstructure. *Mater. Chem. Phys.* **2007**, *101*, 49–55. [CrossRef]

13. Fairhust, W.; Rohrig, K. Abrasion resistant high chromium cast irons. *Foundry Trade J.* **1974**, *136*, 685–698.

14. Filipovic, M.M. Iron-chromium-carbon-vanadium white cast irons—The microstructure and properties. *Hem. Ind.* **2014**, *68*, 413–427. [CrossRef]

15. Pero-Sanz Elorz, J.A. *Ciencia e Ingeniería de Materiales*, 5th ed.; Cie-Dossat: Madrid, Spain, 2006; p. 673.

16. Pero-Sanz, J.A. *Fundiciones Férreas*; Dossat: Madrid, Spain, 1994; p. 154.

17. Gonzalez-Pocino, A.; Alvarez-Antolin, F.; Asensio-Lozano, J. Influence of Thermal Parameters Related to Destabilization Treatments on Erosive Wear Resistance and Microstructural Variation of White Cast Iron Containing 18% Cr. Application of Design of Experiments and Rietveld Structural Analysis. *Materials* **2019**, *12*, 3252. [CrossRef] [PubMed]

18. Wiengmoon, A.; Pearce, J.T.H.; Chairuangsri, T. Relationship between microstructure, hardness and corrosion resistance in 20 wt.%Cr, 27 wt.%Cr and 36 wt.%Cr high chromium cast irons. *Mater. Chem. Phys.* **2011**, *125*, 739–748. [CrossRef]

19. Prat-Bartés, A.; Tort-Martorell, X.; Grima-Cintas, P.; Pozueta-Fernández, L.; Solé-Vidal, I. *Métodos Estadísticos*, 2nd ed.; UPC: Barcelona, Spain, 2004; p. 376.

20. Efremenko, V.G.; Wu, K.M.; Chabak, Y.G.; Shimizu, K.; Isayev, O.B.; Kudin, V.V. Alternative Heat Treatments for Complex-Alloyed High-Cr Cast Iron Before Machining. *Metall. Mater. Trans. A-Phys. Metall. Mater. Sci.* **2018**, *49A*, 3430–3440. [CrossRef]

21. ASTM G76-18. *Standard Test Method for Conducting Erosion Tests by Solid Particle Impingement Using Gas Jets*; ASTM International: West Conshohocken, PA, USA, 2018.

22. Stephens, P.W. Phenomenological model of anisotropic peak broadening in powder diffraction. *J. Appl. Crystallogr.* **1999**, *32*, 281–289. [CrossRef]

23. Karantzalis, E.; Lekatou, A.; Mavros, H. Microstructure and properties of high chromium cast irons: Effect of heat treatments and alloying additions. *Int. J. Cast Met. Res.* **2009**, *22*, 448–456. [CrossRef]

24. Yu, S.K.; Sasaguri, N.; Matsubara, Y. Effects of retained austenite on abrasion wear resistance and hardness of hypoeutectic high Cr white cast iron. *Int. J. Cast Met. Res.* **1999**, *11*, 561–566. [CrossRef]

25. Farah, A.F.; Crnkovic, O.R.; Canale, L.C.F. Heat treatment in high Cr white cast iron Nb alloy. *J. Mater. Eng. Perform.* **2001**, *10*, 42–45. [CrossRef]